

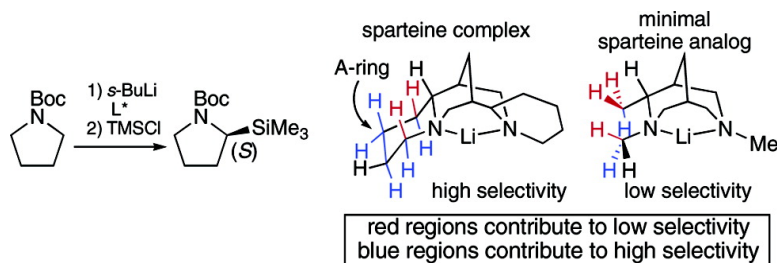
Article

## Is the A-Ring of Sparteine Essential for High Enantioselectivity in the Asymmetric Lithiation–Substitution of *N*-Boc-pyrrolidine?

Puay-Wah Phuan, James C. Ianni, and Marisa C. Kozlowski

*J. Am. Chem. Soc.*, **2004**, 126 (47), 15473-15479 • DOI: 10.1021/ja046321i • Publication Date (Web): 05 November 2004

Downloaded from <http://pubs.acs.org> on April 5, 2009



### More About This Article

Additional resources and features associated with this article are available within the HTML version:

- Supporting Information
- Links to the 5 articles that cite this article, as of the time of this article download
- Access to high resolution figures
- Links to articles and content related to this article
- Copyright permission to reproduce figures and/or text from this article

[View the Full Text HTML](#)

## Is the A-Ring of Sparteine Essential for High Enantioselectivity in the Asymmetric Lithiation–Substitution of *N*-Boc-pyrrolidine?

Puay-Wah Phuan, James C. Ianni, and Marisa C. Kozlowski\*

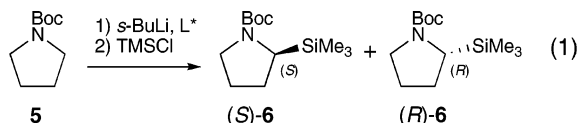
Contribution from the Roy and Diana Vagelos Laboratories, Department of Chemistry, University of Pennsylvania, Philadelphia, Pennsylvania 19104-6323

Received June 22, 2004; E-mail: marisa@sas.upenn.edu

**Abstract:** The simplest chiral portion of sparteine, *N,N*-dimethyl-2-*endo*-methylbispidine, was prepared and evaluated in the asymmetric lithiation–substitution of *N*-Boc-pyrrolidine. The results indicate that the complete A-ring of sparteine is essential for high levels of asymmetric induction. DFT-QSSR analyses of the diamine/Li<sup>+</sup> complexes and DFT calculations of the pertinent *i*-PrLi/diamine/*N*-Boc-pyrrolidine complexes are predictive and provide complementary pictures of the stereochemical features critical to this transformation.

### Background

(–)-Sparteine (**1**; Figure 1), a naturally occurring alkaloid extracted from plants such as Scotch Broom, has proved to be a useful chiral ligand for a wide range of asymmetric reactions.<sup>1</sup> Recently, O'Brien and co-workers<sup>2</sup> reported an elegant synthesis of an abbreviated (+)-sparteine surrogate *ent*-**2**, corresponding to the ABC-rings of the enantiomer of (–)-sparteine. Surrogate *ent*-**2** can attain high enantioselectivity in asymmetric reactions without the D-ring and provides the opposite enantiomer relative to (–)-sparteine. For example, in the asymmetric lithiation–substitution of *N*-Boc-pyrrolidine **5** (eq 1), (–)-sparteine



provides (*S*)-**6** in 96–97% ee,<sup>3</sup> whereas surrogate *ent*-**2** provides (*R*)-**6** in 90–94% ee (Figure 1).<sup>2</sup> Similar trends were observed in several other transformations as well. On this basis, it appeared that the majority of the asymmetric induction supplied by sparteine in this and related transformations was a consequence of the ABC-ring system; the D-ring was concluded to

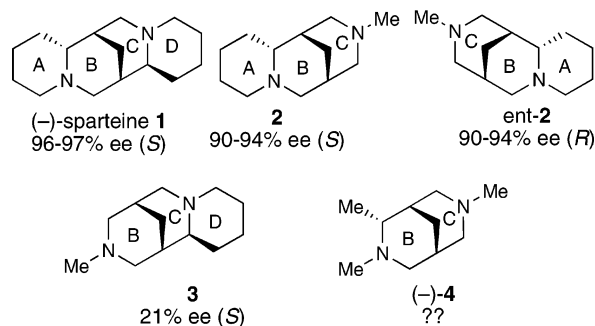
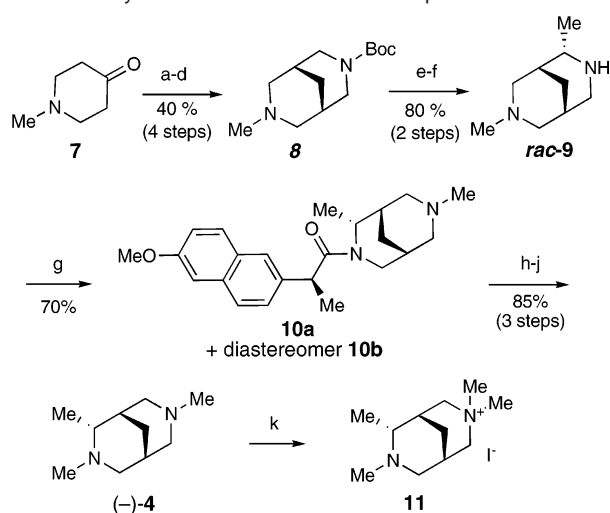


Figure 1.

play a minor role. Silvani and co-workers<sup>4</sup> affirmed this result by preparing diamine **3**, which contains only the BCD-ring of (–)-sparteine. Diamine **3** provides low selectivity (21% ee) in the lithiation–substitution of *N*-Boc-pyrrolidine. The D-ring of **3** did provide a small degree of stereocontrol to the same (*S*) configuration as the A-ring of **2** (matches **3** and (–)-sparteine configuration). Clearly the A- and D-rings act in concert, but the A-ring is the crucial element. The question thus remains, is the entire six-membered A-ring of sparteine essential for achieving a high level of enantioselectivity? To address this question and to elucidate the exact elements of (–)-sparteine responsible for asymmetric induction, we prepared *N,N*-dimethyl-2-*endo*-methylbispidine (**4**) and examined it as a minimal chiral sparteine analogue. The C-methyl group in **4** was proposed to mimic the bispidine substitution afforded by the A-ring of **1** and **2**. The results were examined in the light of two theoretical constructs: (1) a DFT structure/selectivity analysis of diamine compounds employed in asymmetric lithiation–substitution that identifies the asymmetry inducing elements and (2) DFT transition structure calculations.

- (1) For reviews, see: (a) Hoppe, D.; Hense, T. *Angew. Chem., Int. Ed. Engl.* **1997**, *36*, 2282–2316. (b) Beak, P.; Basu, A.; Gallagher, D. J.; Park, Y. S.; Thayumanavan, S. *Acc. Chem. Res.* **1996**, *29*, 552–560.  
 (2) (a) Harrison, J. R.; O'Brien, P.; Porter, D. W.; Smith, N. M. *J. Chem. Soc., Perkin Trans. 1* **1999**, 3623–3631. (b) Harrison, J. R.; O'Brien, P.; Porter, D. W.; Smith, N. M. *Chem. Commun.* **2001**, 1202–1203. (c) Dearden, M. J.; Firkin, C. R.; Hermet, J.-P. R.; O'Brien, P. *J. Am. Chem. Soc.* **2002**, *124*, 11870–11871. (d) Hermet, J.-P. R.; Porter, D. W.; Dearden, M. J.; Harrison, J. R.; Koplin, T.; O'Brien, P.; Parmene, J.; Tyurin, V.; Whitwood, A. C.; Gilday, J.; Smith, N. M. *Org. Biomol. Chem.* **2003**, *1*, 3977–3988.  
 (3) (a) Kerrick, S. T.; Beak, P. *J. Am. Chem. Soc.* **1991**, *113*, 9708–9710. (b) Gallagher, D. J.; Kerrick, S. T.; Beak, P. *J. Am. Chem. Soc.* **1992**, *114*, 5872–5873. (c) Beak, P.; Du, H. *J. Am. Chem. Soc.* **1993**, *115*, 2516–2518. (d) Beak, P.; Kerrick, S. T.; Wu, S.; Chu, J. *J. Am. Chem. Soc.* **1994**, *116*, 3231–3239. (e) Thayumanavan, S.; Lee, S.; Liu, C.; Beak, P. *J. Am. Chem. Soc.* **1994**, *116*, 9755–9756. (f) Gallagher, D. J.; Beak, P. *J. Org. Chem.* **1995**, *60*, 7092–7093.

- (4) Danieli, B.; Lesma, G.; Passarella, D.; Piacenti, P.; Sacchetti, A.; Silvani, A.; Virdis, A. *Tetrahedron Lett.* **2002**, *43*, 7155–7158.

**Scheme 1.** Synthesis of a Minimal Chiral Bispidine<sup>a</sup>

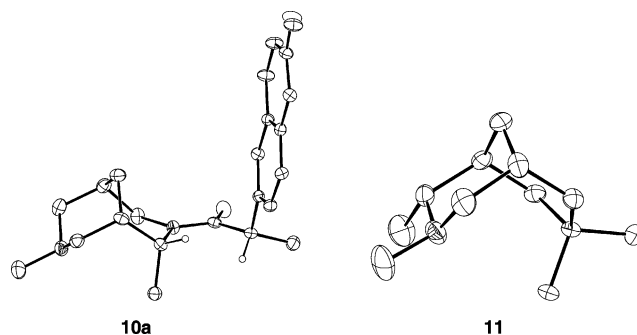
<sup>a</sup> Reagents and conditions: (a) concd HCl, CH<sub>2</sub>O, CH<sub>3</sub>CO<sub>2</sub>H, PhCH<sub>2</sub>NH<sub>2</sub>, MeOH, reflux, 15 h; (b) NH<sub>2</sub>NH<sub>2</sub>·H<sub>2</sub>O, 3 h, 80 °C then, KOH, 160–200 °C; (c) 10% Pd/C, H<sub>2</sub>, 4:1 CH<sub>3</sub>CO<sub>2</sub>H:H<sub>2</sub>O; (d) (*t*-BuOCO)<sub>2</sub>O, CH<sub>2</sub>Cl<sub>2</sub>, rt; (e) Me<sub>2</sub>NCH<sub>2</sub>CH<sub>2</sub>NMe<sub>2</sub>, *s*-BuLi, cyclopentane, MeI, –78 °C, 8 h; (f) CF<sub>3</sub>CO<sub>2</sub>H, CH<sub>2</sub>Cl<sub>2</sub>, rt; (g) (*S*)-(+)-6-methoxy- $\alpha$ -methyl-2-naphthaleneacetic acid, EDCI, CH<sub>2</sub>Cl<sub>2</sub>, rt; (h) CH<sub>3</sub>CO<sub>2</sub>H, concd HCl, 120 °C, 5 h; (i) (*t*-BuOCO)<sub>2</sub>O, CH<sub>2</sub>Cl<sub>2</sub>, rt; (j) LiAlH<sub>4</sub>, THF, reflux; (k) MeI, EtOH.

### Diamine Synthesis and Asymmetric Lithiation–Substitution

By implementing a modified procedure of Waldmann<sup>5</sup> for the first step (double Mannich reaction), sufficient quantities of *N*-Boc-protected bispidine **8** could be prepared from *N*-methylpiperidone **7** (Scheme 1). Lithiation of **8** followed by electrophilic quench with MeI provided the methylated bispidine in good yield.<sup>6</sup> Subsequent trifluoroacetic acid deprotection then provided racemic secondary amine **9** quantitatively. Previous attempts by others<sup>2b</sup> to resolve similar bispidine-type diamines through diastereomeric recrystallization have not been successful. Our strategy thus centered on coupling racemic amine **9** with a chiral auxiliary to give diastereomers that could be separated by simple chromatography. Upon screening a number of *N*-protected amino acids or acids, (*S*)-(+)-6-methoxy- $\alpha$ -methyl-2-naphthaleneacetic acid was found to be the most promising. Coupling of **9** with 2 equiv of this chiral acid and *N*-ethyl-*N'*-(3-dimethylaminopropyl)carbodiimide (EDCI) reproducibly provided amide **10** in good yield (65–70%), and the diastereomers **10a** and **10b** were separated via silica gel chromatography.

Efficient removal of the chiral auxiliary proved to be nontrivial. For example, cleavage with excess of MeMgCl in THF at reflux was sluggish. However, hydrolysis of **10a** in a 1:1 mixture of concentrated hydrochloric acid and acetic acid<sup>7</sup> at 120 °C provided the chiral form in 92% yield after distillation. Subsequent Boc-protection followed by reduction with LiAlH<sub>4</sub> furnished chiral amine (–)-**4**.

The absolute configuration of (–)-**4** was secured from the single-crystal X-ray structure of **10a** using the known absolute stereochemistry of the (*S*)-(+)-6-methoxy- $\alpha$ -methyl-2-naphthaleneacetic acid portion (Figure 2). Further confirmation was

**Figure 2.** ORTEP renderings (30% probability ellipsoids) of **10a** and **11**.**Table 1.** Experimental Results in the Asymmetric Lithiation–Substitution of *N*-Boc-pyrrolidine **5** (Eq 1) with (–)-Sparteine and (–)-**4**<sup>a</sup>

diamine (L* in eq 1)	yield of <b>6</b> (%) <sup>b</sup>	ee of <b>6</b> (%) <sup>c</sup>
(–)-sparteine ( <b>1</b> )	76	95 ( <i>S</i> )
(–)- <b>4</b>	45	35 ( <i>R</i> )

<sup>a</sup> Reaction conditions: (i) 1.3 equiv of *s*-BuLi, 1.3 equiv of diamine, Et<sub>2</sub>O, –78 °C, 5 h; (ii) TMSCl, –78 °C to room temperature overnight. <sup>b</sup> Isolated yield. <sup>c</sup> Enantiomeric excess determined by chiral GC with a Supelco  $\beta$ -DEX 120 capillary column.

obtained via anomalous dispersion from the single-crystal X-ray structure of the corresponding quaternary ammonium iodide salt **11** (Figure 2). The structure of (–)-**4** is analogous to that of (–)-sparteine **1**, where the methyl group of **4** mimics the equatorial disposition of the sparteine A-ring.

With enantiomerically pure (–)-**4** in hand, a direct comparison with (–)-sparteine **1** in the lithiation–substitution of *N*-Boc-pyrrolidine **5** with Me<sub>3</sub>SiCl (eq 1) was undertaken.<sup>3</sup> In accord with prior reports,<sup>2–4</sup> the (*S*) enantiomer of the silylated product **6** was obtained in 95% ee using (–)-sparteine **1** as the ligand (Table 1). Surprisingly, (–)-**4** provided the opposite (*R*) enantiomer of **6** (35% ee). The sense of asymmetric induction was *opposite*, even though diamine (–)-**4** is structurally analogous to (–)-sparteine **1**. The result indicates that **4** is far less selective than sparteine in the asymmetric lithiation–substitution reaction and, more importantly, that the entire A-ring of sparteine is essential for high enantioselectivity.

### QSSR Selectivity Predictions

We have developed a quantitative structure–selectivity relationship (QSSR) protocol to relate the structure of chiral ligands to enantioselectivity in a given transformation. Such<sup>8</sup> methods, which historically predate modern quantum calculations, are advantageous in this type of analysis.<sup>9</sup> For example, information about reaction mechanisms is not needed as long as all the reactions analyzed proceed via the same pathway. Moreover, QSSR calculations are rapid and can provide direct information on the interactions most important to stereochemical induction. To understand the experimental results from diamine **4** and the factors controlling the selectivity for the reaction in eq 1, we undertook QSSR calculations with several diamine lithium complexes.

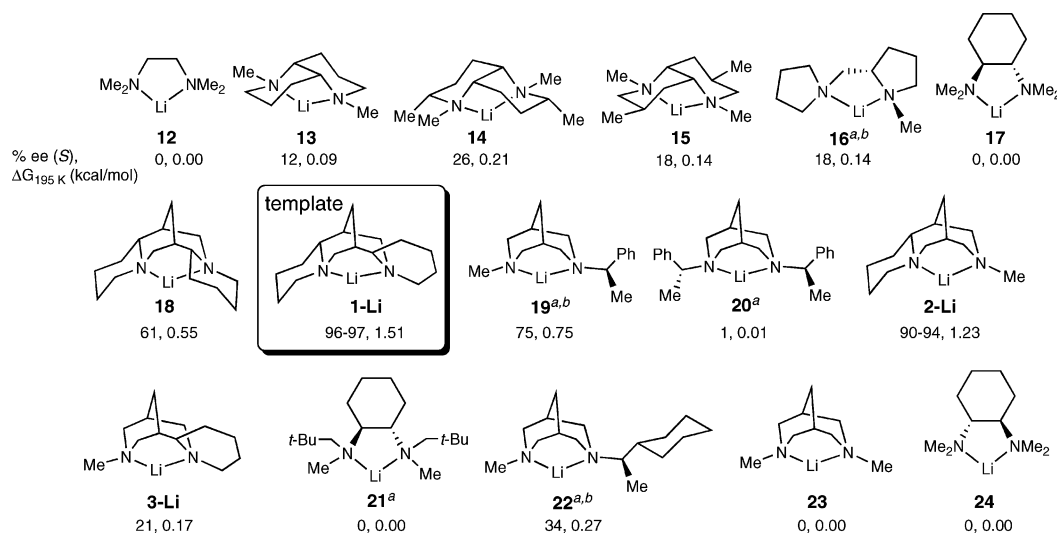
(5) Spieler, J.; Huttenloch, O.; Waldmann, H. *Eur. J. Org. Chem.* **2000**, 391–399.

(6) Harrison, J. R.; O'Brien, P. *Tetrahedron Lett.* **2000**, 41, 6161–6165.

(7) Krasnov, V. P.; Levit, G. L.; Andreeva, I. N.; Grishakov, A. N.; Charushin, V. N.; Chupakhin, O. N. *Mendeleev Commun.* **2002**, 12, 27–28.

(8) For an overview, see: Hansch, C.; Leo, A. *Exploring QSAR. Volume 1: Fundamentals, and Applications in Chemistry and Biology*; American Chemical Society: Washington, DC, 1995.

(9) For the first application of non-CoMFA QSAR type analyses to an asymmetric reaction, see: Oslob, J. D.; Akermark, B.; Helquist, P.; Norrby, P.-O. *Organometallics* **1997**, 16, 3015–3021.

**Chart 1.** Training Set Diamine Lithium Complexes and Their Enantioselectivities from Eq 1 for the Asymmetric Lithiation–Substitution QSSR<sup>c</sup>

<sup>a</sup> The lowest energy conformation of the lithium complex was employed in the QSSR analysis. <sup>b</sup> Two orientations were evaluated in the QSSR analysis. The illustrated orientation gave the best models. <sup>c</sup>  $\Delta G$  values were obtained from  $\Delta G = -RT \ln K$ , where  $K = er$  and corresponds to the differences in energy between two pathways leading to the enantiomeric products.

QSSR entails mathematically correlating the selectivities of a set of catalysts with one or more physical attributes of those catalysts and can be predictive if satisfactory cross-validation is demonstrated. In our case, physical descriptors were obtained by placing each catalyst, oriented in the same way, at the center of a three-dimensional grid<sup>10</sup> and at each grid point evaluating the interaction energy between a probe (a positron) and each aligned molecule. These interaction energies, or electrostatic potential (ESP) fields, were then regressed onto the enantioselectivity data to generate a mathematical model that then can be used to predict the selectivity of new analogues. In undertaking catalyst QSSR analyses, we generated the descriptors quantum mechanically so as to obtain the best possible treatment of the metal components of the catalysts.<sup>11</sup> We have applied this QSSR method to several problems in asymmetric catalysis and obtained very promising results.<sup>11,12</sup> This analysis allows us to infer reactive geometries and to quantify the important links between ligand structure and reactivity–selectivity.

In using this tool to identify the stereochemistry-determining regions of diamines in asymmetric lithiation–substitution, we required experimental data for a range of conformationally well-defined diamine ligands in an asymmetric lithiation–substitution reaction. While a few results have been reported,<sup>2,4,13</sup> we implemented our own program to obtain further data for the lithiation–substitution reaction in eq 1 (Chart 1, **13–15**, **21**).<sup>14,15</sup> Unlike many diamines that have been employed in asymmetric

lithiation–substitution, the limited conformational flexibility of our 1,5-diaza-*cis*-decalins renders them useful for probing the relationship of structure to selectivity–reactivity. With this and other published data,<sup>2,4,13</sup> we generated a QSSR model using the program QM-QSAR,<sup>16</sup> which employs PM3 structures and ESP fields. The structures were aligned using the (–)-sparteine complex **1–Li** as a template by overlaying the Li–N–Li atoms. For non-*C*<sub>2</sub> symmetric compounds, both possible alignments were investigated, and the orientations that ultimately gave the best models are illustrated in Chart 1.

Unfortunately, good models (high  $r_{cv}^2$  values for the input training set) could not be obtained using the QM-QSAR program. We found that the problem lay with the geometries and electron densities obtained at the PM3<sup>17</sup> level that were needed for the ESP calculations; in particular, the calculation was unsuitable for the lithium center. As such, we report here the development of a new program, G-QSAR,<sup>18</sup> which uses the ESP fields generated by Gaussian98 (see Supporting Information). ESP values derived from Hartree–Fock or DFT geometries and the corresponding electron populations provide superior inputs for the QSSR models. Due to the much larger size of the Gaussian molecular orbitals and ESP fields, new methods to compress, align, and extract information from the ESP fields were developed. The new G-QSAR protocol was tested by performing cross-validated analyses of several standard systems and was found to perform better<sup>18</sup> than classic molecular mechanics CoMFA methods and better than the PM3-based QM-QSAR program.<sup>11,16</sup> One particular advantage of the G-QSAR program is that any level of theory (RHF, MP2, B3LYP, etc.), any basis set (3-21G, 6-31G\*, 6-31+G\*\*, etc.),

(10) For an overview, see: Kubinyi, H. In *Encyclopedia of Computational Chemistry*; Schleyer, P. v. R., Ed.; Wiley: New York, 1998; Vol. 1, pp 448–460.

(11) Kozlowski, M. C.; Dixon, S. L.; Panda, M.; Lauri, G. *J. Am. Chem. Soc.* **2003**, *125*, 6614–6615.

(12) Subsequently, two other groups described CoMFA QSAR techniques with respect to chiral catalysts. However, these reports relied on molecular mechanics methods, not necessarily appropriate for organometallic catalysts, and did not describe predictions made prior to an experimental determination. (a) Lipkowitz, K. B.; Pradhan, M. *J. Org. Chem.* **2003**, *68*, 4648–4656. (b) Alvarez, S.; Scheffzick, S.; Lipkowitz, K.; Avnir, D. *Chem. Eur. J.* **2003**, *9*, 5832–5837. (c) Hoogenraad, M.; Klaus, G. M.; Elders, N.; Hooijschuur, S. M.; McKay, B.; Smith, A. A.; Damen, E. W. P. *Tetrahedron: Asymmetry* **2004**, *15*, 519–523.

(13) Gallagher, D. J.; Wu, S.; Nikolic, N. A.; Beak, P. *J. Org. Chem.* **1995**, *60*, 8148–8154.

(14) Li, X.; Schenkel, L. B.; Kozlowski, M. C. *Org. Lett.* **2000**, *2*, 875–878.

(15) Kozlowski, M. C.; Xu, Z.; Santos, A. G. *Tetrahedron* **2001**, *57*, 4537–4542.

(16) Dixon, S. L.; Merz, K. M., Jr.; Lauri, G.; Ianni, J. *J. Comput. Chem.* Accepted.

(17) Dixon, S. L.; Merz, K. M., Jr. *J. Chem. Phys.* **1997**, *107*, 879–893.

(18) Ianni, J.; Kozlowski, M. C. Manuscript in preparation. See the Supporting Information for a description of the G-QSAR program and its implementation.

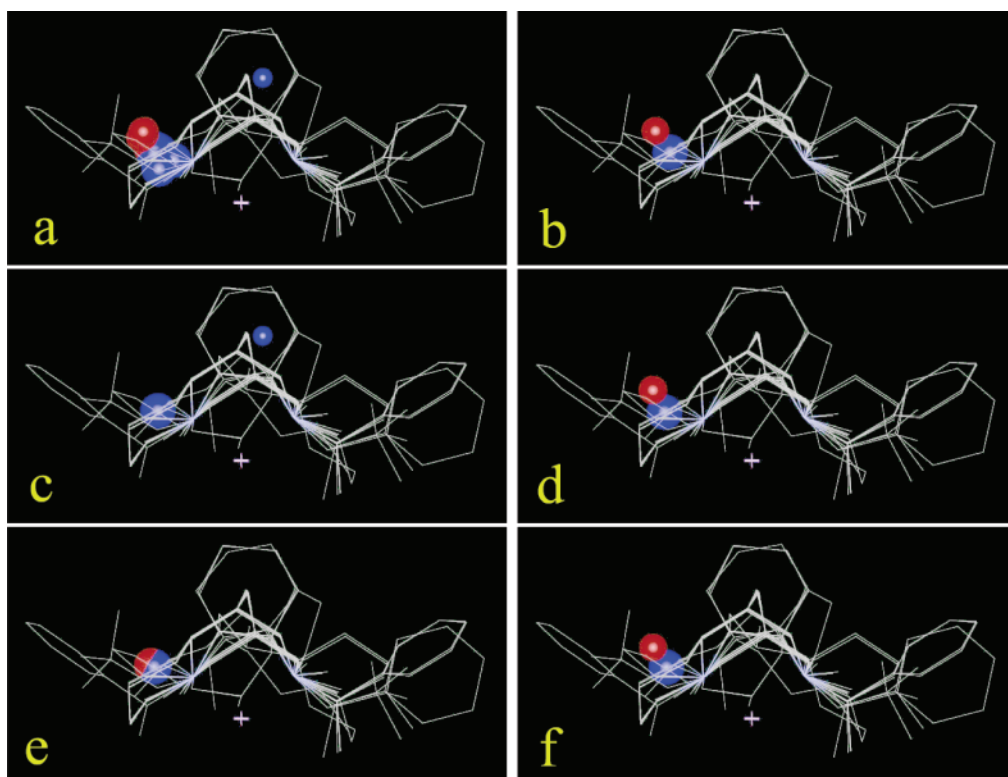


**Figure 3.** Models from the leave-out-one cross-validation of the lithium diamine DFT QSSR. The line structures are the superimposed (via N–Li–N) diamine lithium complexes from Chart 1. Sphere centers represent the probe locations that correlate best with enantioselectivity. Blue = ee increases with increasing probe interaction energy. Red = ee decreases with increasing probe interaction energy. (a) Superposition of all 16 models. (b–f) Five of the 16 models generated in the leave-out-one cross validation.

and any solvent treatment available in Gaussian98 may be employed for the geometries and ESP fields used in the QSSR analyses.

When the G-QSAR program was implemented for the lithiation–substitution of *N*-Boc-pyrrolidine, HF/3-21G\* geometries of the lowest energy conformational isomers of the complexes from Chart 1 and B3LYP/6-31G\*\* ESP fields were employed. Good (high  $r^2$ ) two-point linear regression DFT QSSR models were obtained very quickly. A leave-out-one cross-validation analysis was performed where models were generated using every combination of 15 training set members from Chart 1. Each of these models was then applied to the remaining structure to generate a prediction. The predictions (Table 2) were found to be reasonably good in this analysis with a cross validation  $r^2$  ( $r_{cv}^2$ ) of 0.68 and a correlation coefficient of 0.82. The standard error in these selectivity predictions is 0.27 kcal/mol, which is on the order of that encountered in optimal transition structure calculations.<sup>19</sup> Notably, the different models obtained from the different training set combinations were highly similar (Figure 3). These results indicate that the overall model is robust; minor perturbations of the training set do not create markedly different models.

The probe interaction energies obtained at the centers of the red and blue spheres for each of the diamine–lithium complexes from Chart 1 correlate with the enantioselectivities of the complexes for the reaction in eq 1. Specifically, the probe interaction energy obtained at the center of the blue sphere increased for a given diamine as the enantioselectivity of the

**Table 2.** Experimental vs Predicted Enantioselectivity and  $\Delta G$  Values for the Reaction in Eq 1 Using the DFT QSSR Model

complex	$\Delta G$ (kcal/mol)		% ee	
	expt <sup>a</sup>	pred <sup>a,b</sup>	expt	pred <sup>b</sup>
<b>12</b>	0	−0.032	0	4 ( <i>R</i> )
<b>13</b>	0.093	−0.001	12	0.1 ( <i>R</i> )
<b>14</b>	0.206	−0.199	26	25 ( <i>R</i> )
<b>15</b>	0.141	0.118	18	15 ( <i>S</i> )
<b>16</b>	0.141	0.279	18	34 ( <i>S</i> )
<b>17</b>	0	0.245	0	30 ( <i>S</i> )
<b>18</b>	0.549	0.825	61	78 ( <i>S</i> )
<b>1–Li</b>	1.508	1.502	96–97	96 ( <i>S</i> )
<b>19</b>	0.754	0.214	75	27 ( <i>S</i> )
<b>20</b>	0.008	0.666	1	69 ( <i>S</i> )
<b>2–Li</b>	1.232	1.140	90–94	90 ( <i>S</i> )
<b>3–Li</b>	0.165	0.279	21	34 ( <i>S</i> )
<b>21</b>	0	−0.151	0	19 ( <i>R</i> )
<b>22</b>	0.274	0.460	34	53 ( <i>S</i> )
<b>23</b>	0	0.149	0	19 ( <i>S</i> )
<b>24</b>	0	−0.056	0	7 ( <i>R</i> )

<sup>a</sup>  $\Delta G$  obtained from  $\Delta G = -RT \ln K$ , where  $K = er$  and corresponds to the differences in energy between two pathways leading to the enantiomeric products. <sup>b</sup> Obtained from the leave-out-one cross-validation QSSR analysis for the complexes in Chart 1.

diamine increased. On the other hand, the probe interaction energy obtained at the center of the red sphere decreased for a given diamine as the enantioselectivity of the diamine increased. Factors that cause the probe interaction energy to increase include larger steric bulk (interactions with C–H hydrogens). On the other hand, the probe interaction energy decreases if there are fewer C–H steric interactions or if electrostatic interactions occur with negatively charged groups (i.e., amines, phenyl rings). In this analysis, a two-variable model was found to be sufficient to correlate the structures with the selectivities

(19) For a discussion of the errors in transition structure calculations as they relate to stereoselectivity predictions, see: Bahmanyar, S.; Houk, K. N.; Martin, H. J.; List, B. *J. Am. Chem. Soc.* **2003**, *125*, 2475–2479.

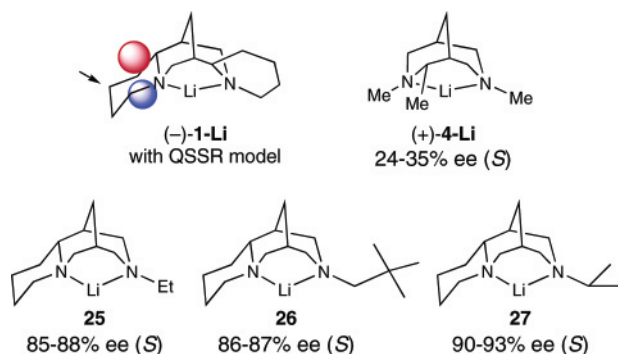


**Figure 4.** Illustration of the DFT QSSR model with the (–)-sparteine–lithium complex. QSSR predictions for the (+)-4–Li complex that yields the same enantiotopic selectivity as (–)-1, as well as for **25–27**, are shown.

(three-point and four-point models did not provide superior regression models). In other words, the structural features in two regions of the chiral diamines, those closest to the illustrated spheres, are most relevant to the stereoselection. As illustrated in Figure 4, these regions are above and below the A-ring of (–)-sparteine. Overall, there is a balance among several effects: (1) larger groups below the ring generally result in higher selectivity, (2) phenyl groups above the ring provide higher selectivity, and (3) larger alkyl groups above the ring cause lower selectivity. From this model, it appears that the methylene group in the A-ring of sparteine (indicated by the arrow in Figure 4) is crucial to the stereoselection.

This model also allows for predictions of new compounds. For (–)-4 from Figure 1, 22–25% ee (*R*) is estimated from the multilinear regression model for the lithiation–substitution of *N*-Boc-pyrrolidine (eq 1). Notably, this prediction indicates that (–)-4 will provide the opposite enantiomer relative to the structurally analogous (–)-sparteine **1**. In other words, the behavior of (+)-4 is expected to be more similar to that of (–)-sparteine (Figure 4). Furthermore, low selectivity is anticipated, indicating that the entire A-ring of (–)-sparteine is indeed critical to asymmetric induction in this class of molecules. Further predictions were also made for a series of analogues based upon O'Brien's complex **2–Li**,<sup>2,20</sup> indicating that the *N*-ethyl (**25**) and *N*-neopentyl (**26**) derivatives should be slightly less selective than **2–Li**, whereas the *N*-isopropyl derivative **27** should exhibit approximately the same level of selectivity as **2–Li** (Figure 4).

### Transition Structure Calculations

To further understand the experimental results from diamine (–)-4, we undertook calculations of the intermediate complexes of *i*-PrLi/4/*N*-Boc-pyrrolidine and the corresponding transition states structures (Figure 5) for the reaction in eq 1. Beginning with the four *i*-PrLi/(–)-sparteine/*N*-Boc-pyrrolidine structures reported by Wiberg and Bailey,<sup>21</sup> (–)-4 was substituted for the sparteine.<sup>22</sup> These four canonical forms were then examined using semiempirical PM3 calculations (Table 3). The two lowest-energy ground-state structures, **B**, leading to removal of

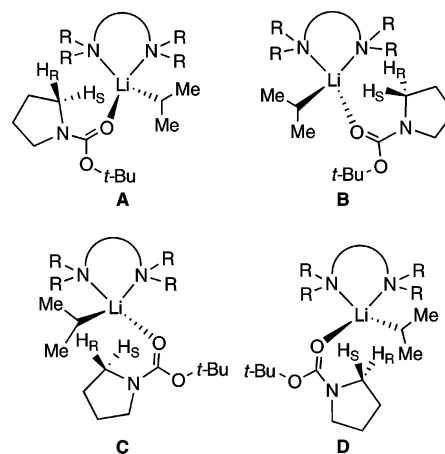


**Figure 5.** Complexes of diamines with *i*-PrLi and *N*-Boc-pyrrolidine.

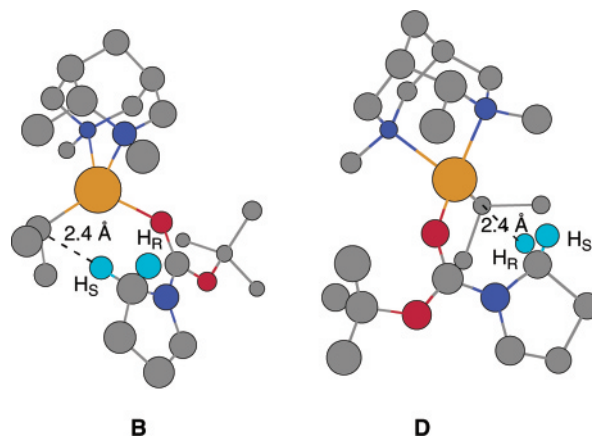


**Figure 6.** Structures of the *i*-PrLi/(–)-4/*N*-Boc-pyrrolidine intermediate complexes **B** and **D** obtained from B3P86/6-31G\*.

**Table 3.** Initial *i*-PrLi/(–)-4/*N*-Boc-pyrrolidine Complexes A–D

	A	B	C	D
<i>i</i> -Pr group	back	front	front	back
pyrrolidine	left	right	left	right
C···H dist (Å)	3.2	3.2	3.0	3.1
PM3 ( $H_f^\circ$ )	–150.227	–154.355	–153.076	–153.987
$E_{rel}$ (kcal/mol)	4.1	0.0	1.3	0.4

the *pro-S* hydrogen, and **D**, leading to removal of the *pro-R* hydrogen, were reoptimized using ab initio HF/3-21G\* and density functional B3P86/6-31G\* methods for more satisfactory energy values.

The energies of geometry-optimized complexes **B** and **D** at the HF/3-21G\* and B3P86/6-31G\* (Figure 6) methods are presented in Table 4. Complex **B** leads to the (*S*) product, while complex **D** leads to the (*R*) product. The calculated distance between the carbonyl oxygen and the deprotonated hydrogens are between 2.5 and 2.8 Å, which brackets the optimal distance of 2.78 Å suggested by Beak.<sup>23</sup> While the difference in the relative B3P86 enthalpies ( $\Delta\Delta H$ ) of complexes (–)-4-**B** and (–)-4-**D** is fairly large (1.40 kcal/mol), the difference in the Gibbs free energies ( $\Delta\Delta G$ ) is very small, favoring the (*S*) product by 0.15 kcal/mol (Table 4, entry 1). A slightly larger free energy difference at 0.85 kcal/mol was found using a HF calculation. In contrast, the corresponding free energy difference reported for (–)-sparteine **15** for the respective complexes is

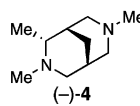
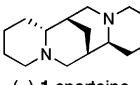
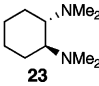
(20) See also the following article in this issue (ja046834p): O'Brien, P.; Wiberg, K. B.; Bailey, W. F.; Hermet, J.-P. R.; McGrath, M. J. *J. Am. Chem. Soc.* **2004**, *124*, 15480–15489 (JA046834p).

(21) (a) Wiberg, K. B.; Bailey, W. F. *Angew. Chem., Int. Ed.* **2000**, *39*, 2127–2129. (b) Wiberg, K. B.; Bailey, W. F. *J. Am. Chem. Soc.* **2001**, *123*, 8231–8238.

(22) For related calculations in the asymmetric deprotonation of achiral alkyl carbamates, see: Würthwein, E.-U.; Behrens, K.; Hoppe, D. *Chem. Eur. J.* **1999**, *5*, 3459–3463.

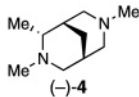
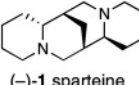
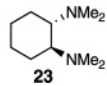
(23) Gross, K. M. B.; Beak, P. *J. Am. Chem. Soc.* **2001**, *123*, 315–321.

**Table 4.** Calculated Energies of *i*-PrLi/(-)-4/*N*-Boc-pyrrolidine Complexes

Entry	Diamine	Calculation	complex		Expt. ee
			D ( <i>pro</i> -R)	B ( <i>pro</i> -S)	
1	 (-)-4	$\Delta\Delta H$ (HF/3-21G*) <sup>a</sup>	0.85	0.00	35% ( <i>R</i> )
		$\Delta\Delta H$ (B3P86/6-31G*) <sup>b</sup>	1.40	0.00	
		$\Delta\Delta G$ (B3P86/6-31G*) <sup>b</sup>	0.15	0.00	
2 <sup>c</sup>	 (-)-1 sparteine	$\Delta\Delta H$ (HF/3-21G*) <sup>a</sup>	3.3	0.00	95% ( <i>S</i> )
		$\Delta\Delta G$ (B3P86/6-31G*) <sup>b</sup>	2.4	0.00	
3 <sup>c</sup>	 23	$\Delta\Delta H$ (HF/3-21G*) <sup>a</sup>	0.5	0.00	0%
		$\Delta\Delta G$ (B3P86/6-31G*) <sup>b</sup>	0.5	0.00	

<sup>a</sup> Difference in calculated total energies, kcal/mol. <sup>b</sup> Corrected for both the differences in ZPE and the change in enthalpy or free energy on going from 0 K (corresponding to the calculations) to 195 K (reaction temperature). <sup>c</sup> From ref 21.

**Table 5.** Calculated Transition Structure Energies for Proton Transfer within the *i*-PrLi/(-)-4/*N*-Boc-pyrrolidine Complexes

Entry	Diamine	Calculation	complex		Expt. ee	Expt. $\Delta\Delta G$ (kcal/mol)
			D-TS ( <i>pro</i> -R)	B-TS ( <i>pro</i> -S)		
1	 (-)-4	$\Delta\Delta G$ (B3P86/6-31G*) <sup>a</sup>	1.3	0.0	35% ( <i>R</i> )	0.28
		$\Delta G^\ddagger$ (B3P86/6-31G*) <sup>a</sup>	12.3	11.1		
2 <sup>b</sup>	 (-)-1 sparteine	$\Delta\Delta G$ (B3P86/6-31G*) <sup>a</sup>	3.2	0.0	95% ( <i>S</i> )	1.41
		$\Delta G^\ddagger$ (B3P86/6-31G*) <sup>a</sup>	12.3	11.5		
3 <sup>b</sup>	 23	$\Delta\Delta G$ (B3P86/6-31G*) <sup>a</sup>	1.2	0.0	0%	0.0
		$\Delta G^\ddagger$ (B3P86/6-31G*) <sup>a</sup>	10.8	10.1		

<sup>a</sup> Difference in calculated total energies, kcal/mol. <sup>b</sup> From ref 21.

much larger 2.4 kcal/mol (entry 2).<sup>21</sup> Furthermore, (*S,S*)-1,2-bis(*N,N*-dimethylamino)cyclohexane **23** (entry 3), another chiral diamine, which gave *racemic* silylated *N*-Boc-pyrrolidine, was calculated to have an energy difference of 0.5 kcal/mol, also slightly favoring the (*S*) product.<sup>21</sup> Thus, on the basis of the calculated energies of ground-state complexes, (-)-4 would be expected to provide substantially less stereoselection in this reaction compared to (-)-sparteine.

The structures of the two lowest energy transition states, **B-TS**, leading to removal of the *pro*-S hydrogen, and **D-TS**, leading to removal of the *pro*-R hydrogen, are depicted in Figure 7. Transition structures for proton transfer within the complexes **B** and **D** were located at the B3P86/6-31G\* level using the synchronous transit-guided quasi-Newton method.<sup>24</sup> The fully optimized transition structures were characterized by one imaginary frequency, which corresponds to the migration of the suitably oriented hydrogen to the *i*-PrLi carbon.

The energy differences between the respective transition state and ground-state complexes (Table 5) of (-)-sparteine **1** and (-)-4 were found to be very similar. For the ground-state

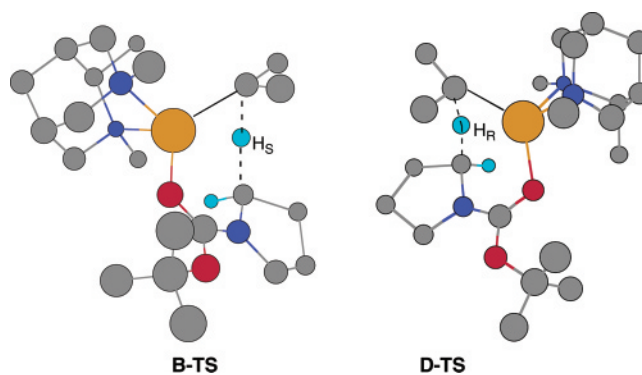


**Figure 7.** Transition state complexes **B-TS** leading to removal of (*pro*-S) hydrogen and **D-TS** leading to removal of (*pro*-R) hydrogen of *N*-Boc-pyrrolidine with diamine (-)-4 (dashed lines indicate transition state bonds).

complex **D** going to transition state **D-TS**, the energy differences are the same at 12.3 kcal/mol for both (-)-sparteine **1** and diamine (-)-4 (Table 5, entries 1 and 2). For the ground-state complex **B** going to transition state **B-TS**, the energy difference is similar, 11.1 kcal/mol for (-)-4 and 11.5 kcal/mol for sparteine **1**. This indicates that the energy differences between the ground-state complexes (i.e. **A-D**) is the predominant factor in determining selectivity. Overall, unselective diamines such

(24) (a) Peng, C.; Ayala, P. Y.; Schlegel, H. B.; Frisch, M. J. *J. Comput. Chem.* **1996**, *17*, 49–56. (b) Peng, C.; Schlegel, H. B. *Isr. J. Chem.* **1994**, *33*, 449–454.

**23**<sup>21</sup> and (–)-**4** displayed energy differences around 1.2–1.3 kcal/mol, while (–)-sparteine **1** has a large difference at 3.2 kcal/mol. In a related report, an energy difference of 1.10 kcal/mol was identified in DFT calculations (B3LYP/6-31G\*) of transition structures for the asymmetric deprotonation of achiral alkyl carbamates by *i*-PrLi in the presence of (*R,R*)-**23**.<sup>22</sup> In contrast to the lithiation of *N*-Boc-pyrrolidine, this transition structure energy difference corresponds quite closely to the observed enantioselection (79% ee, 0.83 kcal/mol) and appears to be the predominant factor in determining selectivity. The reason the DFT calculations only reproduce the *trends* in the lithiation of *N*-Boc-pyrrolidine **5** remains unclear but may arise from the multiple conformational isomers possible, especially with respect to the *tert*-butyl carbamate portion, or be due to solvation effects.

Inspection of transition structures (–)-**4**–**B-TS** and (–)-**4**–**D-TS** reveals that the number of short distances between hydrogens of the diamine lithium complex and the *N*-Boc-pyrrolidine is approximately the same in each of the two structures in contrast to the corresponding (–)-sparteine complexes (more close contacts in (–)-**1**–**D-TS** from the A- and D-rings). Overall, more of these close contacts are observed in the both the corresponding (–)-sparteine structures, especially with the A- and D-rings.

### Concluding Remarks

The simplest chiral portion of (–)-sparteine **1**, diamine (–)-**4**, was synthesized, resolved, and evaluated in the asymmetric lithiation–substitution of *N*-Boc-pyrrolidine **5** (eq 1). Diamine (–)-**4** was found to be much less selective than (–)-sparteine **1** both experimentally and theoretically using DFT QSSR analyses and DFT transition structure calculations. The rapid DFT QSSR analyses completely explain the experimental observations and provide a useful model for locating the stereodiscriminating regions for diamines in this transformation. Notably, the error in these DFT QSSR calculations is small (0.27 kcal/mol), which is competitive with that observed in transition structure calcula-

tions.<sup>19</sup> The transition structure calculations do not fully explain the slight predominance of the (*R*) product in the asymmetric lithiation–substitution of *N*-Boc-pyrrolidine when employing (–)-**4** as the ligand but are consistent with the low observed stereoselection. Accounting for the entire array of minor conformational variants or a higher level theoretical treatment of transition structures might be needed to fully explain the experimental observations. Overall, the DFT QSSR and the DFT transition structure calculations are complementary, with the former identifying important stereodetermining elements and the latter providing an assessment of the bonding changes and energies. We have definitively shown that the entire A-ring of sparteine **1** is a prerequisite for high enantioselectivity in the lithiation–substitution reaction of *N*-Boc-pyrrolidine **5**, and it is likely that this feature is crucial in other asymmetric reactions conducted with sparteine.

**Acknowledgment.** Financial support of this research was provided by the National Institutes of Health (GM59945) and the Alfred P. Sloan Foundation in the form of a Research Fellowship (M.C.K). Computing support was provided by the NCSA in the form of a supercomputing grant. The invaluable assistance of Dr. Patrick Carroll in obtaining the X-ray structures is gratefully acknowledged. We thank Prof. Kenneth Merz for making available to us the DivCon and QM-QSAR programs prior to their release. We are grateful to Steven Dixon and Giorgio Lauri for helpful discussions regarding QSAR analyses. We thank Peter O'Brien for providing the structures of **25**–**27** prior to publication.

**Supporting Information Available:** Full experimental details are provided, including characterization of all synthesized compounds, detailed descriptions of the computational methods, and coordinates of calculated structures. This material is available free of charge via the Internet at <http://pubs.acs.org>.

JA046321I